Behavior of Circular and Square Monopile Structures Installed in Normally Consolidated Clays

Behrang Pedram
Department of Civil Engineering–University of Rahman Ramsar, Ramsar, Mazandaran/Iran

ABSTRACT
This paper investigates the stiffness and ultimate lateral capacity of circular and square pile/tower configurations with equal cross sectional areas installed in normally consolidated clays at shallow water depths. Three-dimensional numerical models are constructed for both pile/tower configurations. The piles are modeled as elastoplastic materials, while the soil is idealized using the Tresca failure criterion with a linearly increasing soil modulus. The undrained shear strength is related to the overconsolidation ratio and the effective vertical stress within the soil medium. The ultimate lateral capacities and the location of the maximum bending moments generated on the hollow pile/tower structures calculated from the numerical analyses are compared with the available solutions in the literature.

RÉSUMÉ
Ce papier enquête sur la raideur et la capacité latérale ultime de configurations de tas/tour circulaires et carrées avec les régions à éléments fâchées égales installées dans les glaises normalement unies pour les profondeurs peu profondes d'eau. Les modèles numériques en trois dimensions sont construits pour les deux configurations de tas/tour. Les structures de tas sont considérées comme elastoplastic le matériel, pendant que le sol est idéalisé en utilisant le Tresca constitutive le modèle avec un module de sol d'une façon linéaire augmentant. En outre, la force de tondage non égouttée est rattachée au rapport de surconsolidation et à la tension verticale efficace dans le médium de sol. Les capacités latérales ultimes et l'endroit des moments de torsion maximums produits sur les structures de tas/tour creuses calculées des analyses numériques sont aussi par rapport aux solutions disponibles dans la littérature.

1 INTRODUCTION

As renewable energy sources become more attractive, larger wind turbines are used to capture a greater amount of energy per structure. This leads to higher lateral and moment loads being imposed on the foundation. It is customary to use hollow circular steel tubes for offshore wind turbines, similar to the Egmond aan zee and the Horns rev wind farms constructed in Europe in 2006 and 2002 respectively. This paper investigates the lateral response of monopiles embedded in normally consolidated clays at shallow water depths with two different pile configurations to improve the behavior of such structures in practice.

In recent years, many structures have been proposed and extensively investigated to replace or enhance the response of monopile foundations. Some of these proposed structures are tripod foundation systems, piled footings (Dixon 2005, Stone et al. 2007 and Pedram 2018), un-piled footings (Byrne et al. 2002) and suction caissons (Houlsby et al. 2005). However, the benefits of these proposed structures are illustrated, in practice many onshore and offshore wind farms are still constructed by monopile foundations, similar to the London Array offshore wind farm constructed off the Kent coast in the United Kingdom in 2013.

Reese (1958), Matlock (1970), Broms (1964), Poulos (1971), Randolph and Houlsby (1984), Fleming et al. (1992), Davies and Budhu (1986) and Murff and Hamilton (1993) have investigated the response of a single pile embedded in a clay layer. Some of these studies emphasis on the stiffness of the monopile structure (Poulos 1971) while others focus on the ultimate lateral capacity of the pile structure embedded in a clay layer (Broms 1964 and Murff and Hamilton 1993).

Figure 1 is a schematic illustration of an offshore wind turbine with the applied loads acting on the structure. In this study two different pile/tower configurations are installed in two normally consolidated clay deposits with a shallow water depth of 5 m. The two nominated pile/tower configurations have a circular and square cross section. Furthermore, as the costs of construction and transportation can significantly influence the design parameters, the volume of the two nominated pile/tower configurations are adjusted so that they use the same amount of material. This allows for an appropriate comparison between the two structures embedded in the normally consolidated clay layers. This is considering the concept of optimum design discussed by Ugural (2007); the concept states that optimum design is the best solution within given constraint(s), such as minimum weight or volume and minimum cost. Due to this consideration the moments of inertia of the pile structures are not equated.

Offshore marine deposits are typically normally consolidated (Wang et al. 2008) with the undrained shear strength (s_u) increasing linearly with depth. This is a typical case of offshore marine clays in South Korea. In the numerical analyses, the soil is normally consolidated while the pile/towers are elastoplastic and a static load is applied to the tower heads. Moreover, the ultimate lateral capacities of the pile/tower structures calculated from the numerical models are checked with respect to the theoretical solution of Murff and Hamilton (1993).

Many pile engineers only consider the stiffness of such structures in practice, it is crucial to study the ultimate lateral capacity of monopiles as well. The significance of calculating the ultimate lateral capacity of monopiles in cohesionless soils is discussed and investigated by Pedram (2015). By applying a static load

on the tower head it is illustrated which component, that is the structure or the soil is likely to fail under a lateral loading scenario.

As discussed, these pile/tower structures are usually designed with respect to their stiffness as the electrical and mechanical devices within the nacelle can sustain small amount of displacements. Due to this criterion the structures are designed for their stiffness and for small amount of displacements, consequently the effect of stress concentrations which are generated at high stress levels is not appropriate for square pile/tower structures.

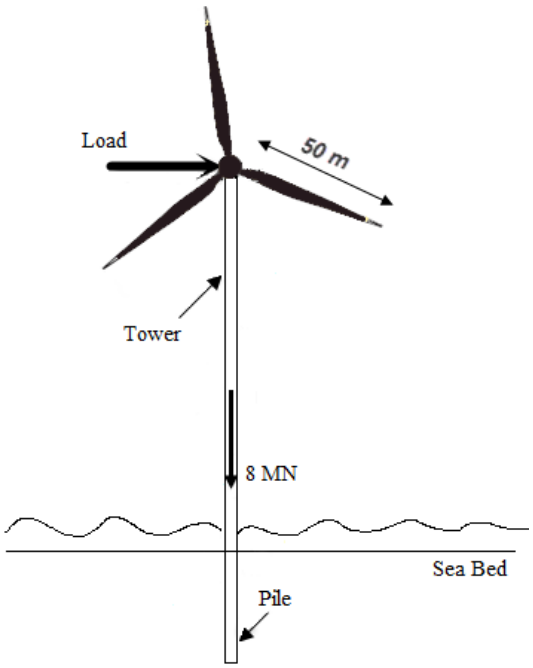

Figure 1. A schematic illustration of an offshore pile/tower structure (not to scale)

2 METHODOLOGY

2.1 Soil Characteristics

The three dimensional finite element analyses are carried out wby ABAQUS (Dassault Systèmes). The soil is idealized using the Tresca constitutive model with a linearly increasing modulus of elasticity. As illustrated by Poulos and Davis (1980) the modulus of elasticity (kN/m^2) of clays for driven piles are in the range of 250-500 × s_u (kN/m^2). Moreover, the shear strength of a clay layer is related to its effective vertical stress and the overconsolidation ratio through $s_u = 0.22 \times \sigma_v' \times OCR$ (Mesri 1975), where σ_v' is the effective vertical stress and OCR is the overconsolidation ratio of the clay deposit. The soil properties for the two clay layers in the numerical models are illustrated in Table 1.

The value of the earth pressure (K_0) in Table 1 is calculated from $(1 - \sin(\phi_{cr}')) \times (OCR)^{0.5}$ (Meyerhof 1976) with $\phi_{cr}' = 0^o$ and OCR = 1. A Python script increased the soil's modulus of elasticity and the undrained shear strength for each individual numerical model as in Table 1 from the ground level. A very small value is required for the modulus of elasticity and the undrained shear strength at the ground level for the numerical models to initiate the calculation. Furthermore, the analyses are performed using a full Newtonian scheme. ABAQUS adopts a Von Mises flow rule with the Tresca failure criterion, in order to avoid problems in defining the relative plastic strain magnitudes at the vertices of the hexagonal failure criterion.

Table 1. Mechanical properties of the adopted soils

Soil Properties	**Soil Group A**	**Soil Group B**
Effective unit weight	7 kN/m^3	7 kN/m^3
Undrained shear strength (kPa)	0.22×σ′×OCR	0.22×σ′×OCR
Modulus of Elasticity (kPa)	350 s_u (kPa)	500 s_u (kPa)
Poisson ratio	0.49	0.49
Earth pressure (K_0)	1	1
Dilatation angle (ψ)	0^o	0^o

2.2 Pile/Tower Characteristics

The pile/towers in this study are constructed out of steel with yield strength of 355 MPa. A low percentage of carbon is required for steels if they are to maintain a high degree of resilience and toughness; this allows the alloy to enter the cold working region (strain hardening). The modulus of elasticity of steel does not significantly alter as the percentage of carbon is changed for different steel alloys (Hibbeler 2005), so a constant value of 200 GPa is suitable for the numerical analyses. Furthermore, the initial monopile dimensions in this study are adopted from the Egmond aan zee wind farm constructed off the Dutch coast in the North Sea in 2006.

Fig. 2 illustrates the stress versus strain graph (engineering) for steel S355 MC, which is used for constructing monopile structures in practice. The material is ductile and its yield point is at 394 MPa. The mechanical properties in the numerical models for the steel monopile structures are illustrated in Table 2. In all numerical models, the yield point of steel S355 MC is equal to 355 MPa. This value is equivalent to the proportional limit of the metal (10% less than the yield stress). A Von Mises yield criterion was adopted for the pile structures in the numerical models as steel S355 MC is a ductile material and this yield criterion is well suited for such materials.

Table 3 provides the initial dimensions for the circular pile/tower structure. For the square structure, the outer breadth is equal to the outer pile diameter. The concept of equating the outer pile diameter with the outer breadth is well established and considered by scholars such as Budhu and Davies (1987).

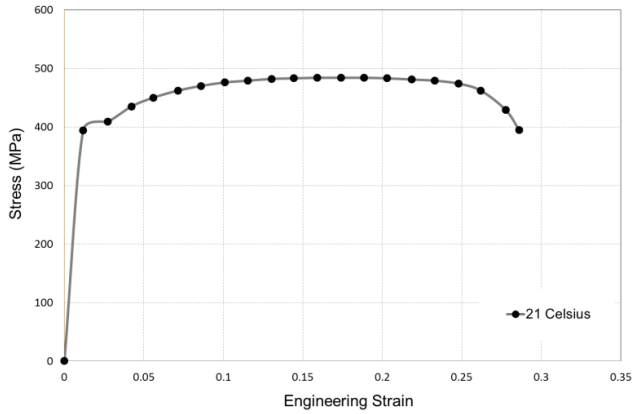

Figure 2. Stress versus strain diagram for steel S355 MC

Table 2. Mechanical properties of steel S355 MC

Unit weight	78 kN/m^3
Modulus of Elasticity	200 GPa
Poisson ratio	0.32
Yield strength	355 MPa

Table 3. Pile/tower dimensions adopted in the numerical models

Pile length under the ground	30 m
Tower length or pile eccentricity	90 m
Outer pile diameter	4.6 m
Inner pile diameter	4.48 m
Pile thickness	60 mm

2.3 Steps, Interactions, Loads and Boundary Conditions

For all numerical models, three steps are required. The first step is to apply the gravity load to the entire model (soil and the pile/tower structure) while in the second step a vertical load of 2.5 MN is applied to the tower head and in the third step the tower's head is laterally displaced.

All parts (soil block and the pile/tower) in the numerical models were tied to each other with respect to the mesh density allocated to each part instance. By tying the parts to each other in the numerical models any extraneous shear stress, which would have occurred after applying the gravity load was avoided. Furthermore, the pile-soil contact was fully rough in shear and fully bounded in tension.

The weight of the nacelle, hub and rotor acting on the pile/tower in the numerical models is 2.5 MN. This load is changed to a pressure and is applied to the tower's head for both pile/tower configurations in the numerical models. Moreover, a water depth of 5 m is adopted for all constructed models; this meant that the buoyant unit weight of steel is adopted for the pile structures up to a height of 5 m above the ground level. Furthermore, only the effective unit weight of the soil is used in the analysis (Table 1).

All numerical models have reflective symmetry and so three boundary conditions are required for the soil block. The soil block and the circular pile/tower structure with the applied loads are illustrated in Fig. 3. The base of the soil block is restricted from moving in the vertical direction; the radial region of the soil is restricted from moving in both horizontal directions while the front face of the soil is restricted from moving normal to the plane of symmetry. The fourth boundary condition is applied to the tower's head in the third step of the analysis as the models are displacement controlled. By applying a boundary condition to the entire tower head, any localized deformation that would take place due to applying a force at a particular point on the tower is avoided. By applying a boundary condition to the tower head, the lateral deflection versus the lateral load graph can be generated, as the summation of all nodal forces located on the tower head is equivalent to the lateral force. Moreover, displacement solutions are more accurate than stress solutions (Cook et al. 2002).

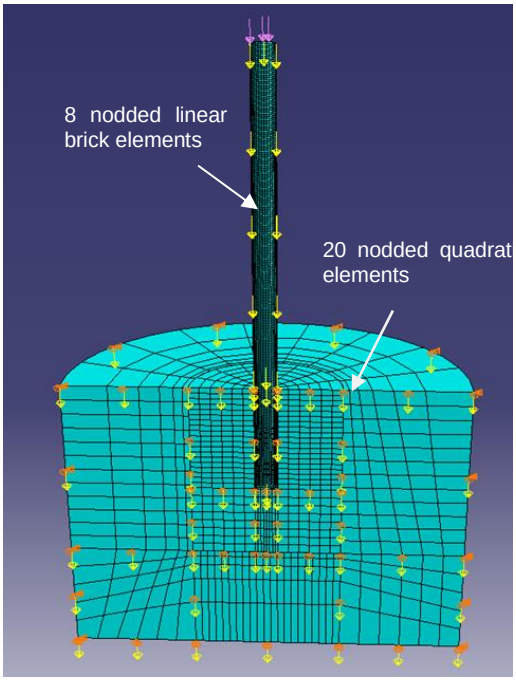

Figure 3. The soil block and the circular pile/tower structure

2.4 Mesh Details

The soil block had large dimensions (over five times the radius of the pile structure) so that the displacements and stresses within the elements became significantly small at locations far from the foundation load. Fig. 3 also illustrates the mesh generated on a model with a circular pile/tower structure.

A semicircular soil block is adopted for all numerical models in this paper as higher order elements can be used on such a soil body configuration. The mesh on the soil block contains 20 nodded brick elements. Cook et al. (2002) and Logan et al. (2011) mention that higher order elements rapidly converge to their exact solutions without an extremely fine mesh (see Logan et al. 2011 page 507, Table 11-2). The pile/tower's mesh contains 8 nodded linear brick elements with a reduced integration and hourglass control scheme. Cook et al. (2002) discuss that a reduced integration scheme can improve the accuracy of the results.

2.5 Adopted Pile Configurations

The effects of the pile/tower's shape on the stiffness and ultimate lateral capacity for the structures are investigated. The hollow circular configuration is changed to a square for comparison purposes. As the costs of constructing and transporting the structures are of a great importance, the dimensions of the nominated pile shape (square) is adjusted so that its surface area is equal to the initial hollow circular pile/tower structure used in the Egmond aan zee wind farm. Moreover, the pile/tower lengths for both configurations are kept as in the initial design (Table 3). The most efficient design can be adopted for these structures by using the same amount of material for both pile/towers (i.e. the concept of optimum design, Ugural 2007). The moments of inertia for the structures are not equated as it is not a requirement for the concept of optimum design. Furthermore, as discussed, the square structure has an outer breadth of 4.6 m (equal to the outer diameter of the circular pile) and an inner breadth of 4.506 m (thickness of 47 mm).

3 THEORETICAL SOLUTION

Reese (1958), Broms (1964), Matlock (1970) and Murff and Hamilton (1993) use different methods for calculating the ultimate lateral capacity of a single pile structure embedded in a clay layer. The numerical results obtained in this study are compared with the method adopted by Murff and Hamilton (1993).

Murff and Hamilton (1993) propose equations 1 through 3 for calculating the ultimate lateral capacity of a single pile embedded in a clay layer.

$$P_u = \left(N_p s_u + \sigma'_v\right) D_p \quad [1]$$

$$N_p = N_{pl} - \left(N_{pl} - 2\right) e^{\frac{\xi z}{D_p}} \quad [2]$$

$$\xi = 0.25 + 0.05 \left(\frac{s_{u0}}{D_p k}\right) \leq 0.55 \quad [3]$$

In the above equations P_u is the limiting force per unit length of the pile, s_u is the undrained shear strength of the soil, σ_v' is the effective vertical stress in the soil, D_p is the pile diameter (or breadth), N_p is a factor expressed as a function of Z (depth) and ξ (Eq. 3). Moreover, s_{u0} is equal to the undrained shear strength of the soil at the ground level while k is the slope of the variation of s_u with depth (Z).

Randolph and Houlsby (1984) provide the value of N_{pl} for a rough circular pile as 11.94 while Poulos and Davis (1980) provide a value of 11.14 for a rough square pile configuration. Furthermore, Broms (1964) suggests a value of 9.0, which can also be used in Eq. 2. In this paper, the values of 11.94 and 11.14 are considered for the circular and square pile/towers respectively.

If the theoretical solutions are to be compared with the numerical results; in Eq. 1 the value of s_u must alter with the effective vertical stress in the soil medium as in $0.22 \times \sigma_v' \times OCR$ (Mesri 1975). This also ensures that a value of 0.25 can be considered for ξ (Eq. 3).

For calculating the ultimate lateral capacity of a single pile structure embedded in a soil layer it is conventional to evaluate the bending moment at the pile's toe symbolically with respect to the adopted soil resistance and then to evaluate the ultimate lateral capacity (H_u) by rearranging the terms in moment equation. The location of the maximum bending moment (*f* (m)) along the pile's length is calculated by considering the shear forces to be zero at a certain depth under the ground. The maximum bending moment (M_{max}) is evaluated symbolically at that depth with respect to the adopted soil resistance. The pile status (short or long) is identified by comparing, the values of M_{max} with M_{yield} (calculated from the flexure equation). If $M_{max} < M_{yield}$ the pile is short and the ultimate lateral capacity is calculated from the equation derived symbolically for the pile's toe. If $M_{max} > M_{yield}$ the pile is long (structural failure) and the ultimate lateral capacity is calculated from the equation derived for M_{max} with $M_{max} = M_{yield}$. The equations are solved for the two unknowns (*f* and H_u) with two equations; unfortunately, for the adopted soil resistance provided by Murff and Hamilton (1993) with the undrained shear strength to increase as in $0.22 \times \sigma_v' \times OCR$, the two equations cannot be solved.

The best way to surpass the problem is to break the pile's length into small segments and to evaluate the location of the plastic hinge through iteration by a script. Such a script can identify the location of the maximum bending moment, the ultimate lateral capacity of the pile structure and its status (short or long). For long piles, the lateral soil resistance behind the pile section is neglected as the location of the maximum bending moment occurs above the pile's point of rotation. A MATLAB script was generated, which followed the discussed procedure.

4 RESULTS AND DISCUSSION

Fig. 4 illustrates the results of the circular and square pile/tower configurations embedded in soil groups A and B. It is clear that for both soil groups, the stiffness of the square structure is higher than of a circular pile/tower. Furthermore, from Fig. 4 it is evident that the ultimate lateral capacities of both structures are equal.

From Fig. 4 it is not clear which component, that is the soil or the pile/tower structures fail at 3.0 MN.

To identify which component initially fails in the FE models, the Tresca criterion is removed from the soil structure; that is the soil is changed to an elastic medium while the pile/towers are still acting as an elastoplastic material. Figs. 5 and 6 illustrate the results of this analysis.

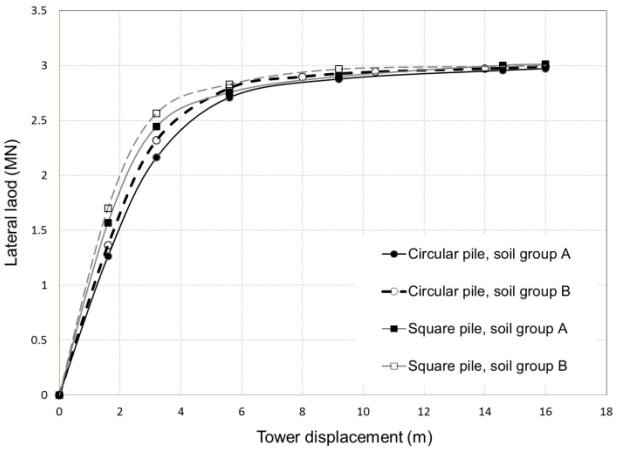

Figure 4. Lateral load-deflection behavior of the monopiles embedded in soil groups A and B

From the results of Figs. 5 and 6 it is clear that soil failure controls the ultimate lateral capacity of both structures embedded in soil groups A and B. Both pile configurations embedded in soil groups A and B are classified as short (soil failure). Furthermore, form Figs. 5 and 6 it is evident that if structural failure controls the ultimate lateral capacity of the pile/tower structures, the square pile/towers provide a higher ultimate capacity and stiffness compared to a circular structure embedded in both soil groups.

The generated MATLAB script, which followed the method adopted by Murff and Hamilton (1993), predicts that the ultimate lateral capacities of the circular and square pile/tower structures are equal to 3.1 and 3.02 MN respectively. As discussed, the value of N_{pl} is equal to 11.94 and 11.14 for the circular and square pile/tower structures respectively. The FE results calculate a value of 3.0 MN for the circular and square pile/tower structures at large tower head displacements, which is in a very close agreement with the theoretical solution. It must also be pointed out that the method of Murff and Hamilton (1993) considers the pile structures to be short as in the case of the numerical models, i.e. the ultimate lateral capacity is controlled by soil failure and not by the structural capacity of the pile/towers.

Broms (1964) states that the maximum resistance is in general reached when the deflection at the ground surface (not the tower head displacement as is illustrated in Fig. 4) is approximately equal to 20% of the diameter or side of the pile. The tower head displacements where altered so that a displacement of 0.92 m (20% of the pile diameter) was captured for the circular pile structures embedded in soil groups A and B at the ground level (not illustrated). At a deflection of $0.2D_p$ at the ground level (this equates to a tower head displacement of 6.7 m for soil group A and 6 m for soil group B in Fig. 4 for the circular structures) the circular pile structures provide a value of 2.82 MN for soil groups A and B. This illustrates that the deflection criteria set by Broms (1964) for the ultimate capacity is well suited for large pile diameters used in offshore practice.

It is interesting to note that Eqs. 4 and 5 developed by Davies and Budhu (1986) (or Budhu and Davies 1987) predict that the circular pile structures behave as intermediate piles with respect to their stiffness. In Eqs. 4 and 5, E_p is the modulus of elasticity of an equivalent solid pile section, D_p is the pile diameter and m is the rate of increase in Young's modulus with depth (N/m^3). For Eq. 4, an equivalent value of E_p is used as the equations are originally derived for a solid circular pile section and not for a hollow circular structure ($E_{p,equivalent} = E_{p,actual}\ (r_o^4 - r_i^4)/r_o^4$, which r_o and r_i are the outer and inner radius respectively). By adopting $E_{p,equivalent}$ (20 GPa) and considering m equal to 539 and 770 kN/m^3 for soil groups A and B respectively, the effective pile lengths (Eq. 5) are equal to 44 m and 40.7 m for soil groups A and B respectively. This illustrates that for the circular pile structures embedded in both soil groups their stiffness can be further increased if the pile lengths are enlarged.

$$K = \frac{E_p}{mD_p} \quad [4]$$

$$L_a = 1.3 D_p K^{0.222} \quad [5]$$

From the results of Fig. 4 it is apparent that the ultimate lateral capacities of the square and circular structures are equal as soil failure controls the ultimate lateral capacities. The stiffness of the square structures are higher than the circular pile/towers embedded in both soil groups. For example, in soil group A at a tower head displacement of 0.23 m, which equates to $0.05D_p$ (D_p is the pile diameter or pile breadth) the difference calculated between the stiffness of the two structures is equal to +18.4%. Furthermore, at a tower head displacement of 0.46 m, which equates to $0.1D_p$ the difference in the stiffness is equal to +26.31%. In soil group B the difference in the stiffness for a pile head displacement of 0.23 m between a square and circular structure is equal to +30.0% while at a tower head displacement of 0.46 m that difference is equal to +32.2%. This clearly illustrates that the stiffness of the square pile/tower structure is higher than of a circular structure with the same volume of material used for constructing both structures. The higher stiffness of the square structures is attributed to its higher side shear resistance.

Fig. 7 illustrates the lateral stresses acting on the soil body at the center of the pile's cross section in the direction of the applied displacements to the tower's head. It is apparent that at the pivot point depth, the lateral stresses acting on the soil body along the pile shafts are zero.

Both clays considered in this study are normally consolidated and consequently soil failure controls the ultimate lateral capacities. If a higher overconsolidation ratio (OCR ≥ 2), is considered in Table 1 as in an onshore scenario, it is likely that the structural capacity of the pile/tower structures control the ultimate capacities. If the latest point is to be considered in the analysis, from Figs. 5 and 6 it is evident that the stiffness and the ultimate lateral capacities of the square structures embedded in both soil groups are higher than of a circular pile/tower with the same amount of material used for constructing both structures. As previously mentioned, the higher stiffness of the square structure is due to the side shear resistance of the pile configuration. In a circular pile, the

curvature decreases the amount of drag between the soil and the structure. Note that even when the moments of inertia of the pile structures are equated, the stiffness of a square pile stands higher than of a circular structure due to the effects of drag between the sides of the square structure and its surrounding soil.

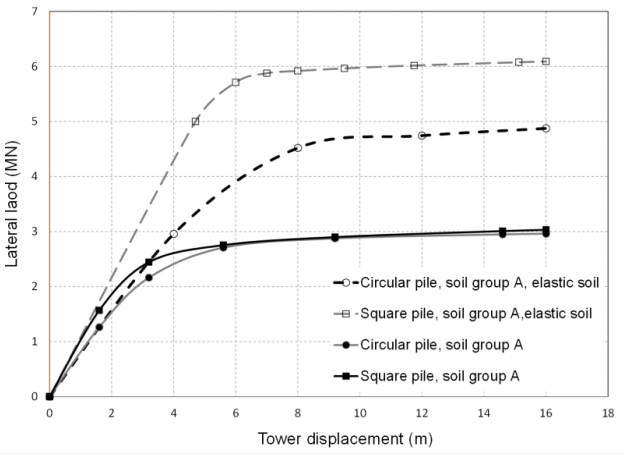

Figure 5. Lateral load-deflection behavior of monopiles embedded in soil group A

As discussed by API (American Petroleum Institute) the frequency of occurrence of specified wind speeds from various directions for each month or season must be gathered before erecting the pile/tower structures (i.e. the recommended site is investigated for at least one year to define the direction of the strongest wind speed before erecting such structures in practice). It is clear that for wind turbines, the rotor must be installed in the direction of the strongest specified sustained wind speed, this means that at least a 50 m blade (Fig. 1) cuts through the direction of the strongest wind acting on the structure and consequently it removes a significant portion of the drag imposed by the wind on such structures. That is the effect of the wind drag on the structure is substantially removed for the square pile/tower structure.

It is important to generate the bending moments acting on the circular pile/tower structure and to identify the location of the maximum bending moment. Moreover, the location of the maximum bending moment generated from the FE models is compared with respect to the results obtained from the theoretical method adopted by Murff and Hamilton (1993). In finite element analysis a wire or a beam element must be installed at the center of the pile structure with a modulus of elasticity, which is a million times less than the pile to generate the bending moment acting on the structure. The diameter or breadth of the embedded beam element must also be equal to the outer diameter or outer breadth of the circular or square pile structures respectively. As the circular pile/tower structures in this study are both hollow, a beam element cannot be installed at the center of the pile/tower structures. To overcome this problem, a solid pile/tower is generated so that a beam element could be embedded into the structure's body. To construct a solid pile/tower, the moduli of elasticity of the hollow and solid structures are equated as in Eq. 6 to calculate an equivalent modulus of elasticity for the solid pile/tower. Furthermore, the equivalent density (ρ) is also calculated through Eq. 7 with respect to the surface area of the pile/tower section. In Eqs. 6 and 7, E_p is the modulus of elasticity of the pile, I is the second moment of inertia of the pile structure, ρ is the pile density and A is the cross sectional area of the structure.

By using the equivalent modulus of elasticity and density, a solid pile/tower is constructed and the dimensions of the beam elements embedded at the center of the structures are adjusted with the outer diameter. As the length of the pile/tower is more than 10 times its outer diameter, the transverse shear deformation can be neglected in the analysis (Logan et al. 2011).

Fig. 8 illustrates the bending moments generated on the circular pile/tower embedded in soil group B at the ultimate lateral capacity and at a tower head displacement of 0.46 m ($0.1D_p$). It must be noted that the bending moments were extracted by the aid of MATLAB and the Python script.

The location of the maximum bending moment acting on the circular pile/tower is 8.8 m below the ground level. The location of the maximum bending moment calculated from the theoretical method adopted by Murff and Hamilton (1993) is 9.6 m below the sea level. It must be reminded that for the circular pile/tower configuration N_{pl} is equal to 11.94 in the theoretical equation.

Form Fig. 8 it is apparent that the location of the maximum bending moment generated along the circular pile/tower structure increases as the structure moves towards its ultimate lateral capacity. Davies and Budhu (1986) also observed this point in their analysis. This meant that as the load on the structure increases, not only the magnitude of the bending moment rises, but also the depth of the maximum bending moment increases as well. The location of the maximum bending moment at a tower head displacement of 0.46 m ($0.1D_p$) occurred at a depth of 3.75 m below the sea level, as illustrated in Fig. 8.

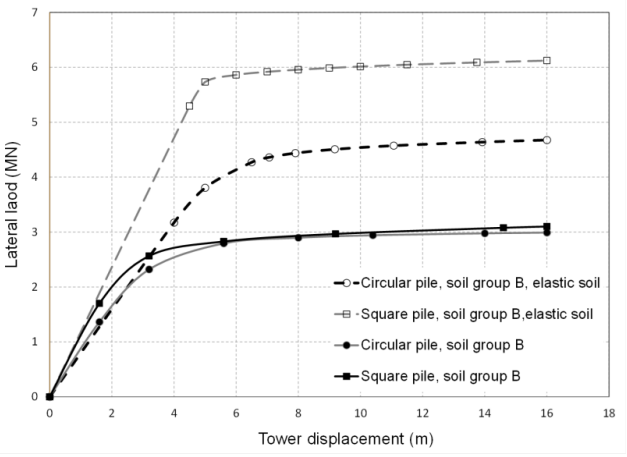

Figure 6. Lateral load-deflection behavior of monopiles embedded in soil group B

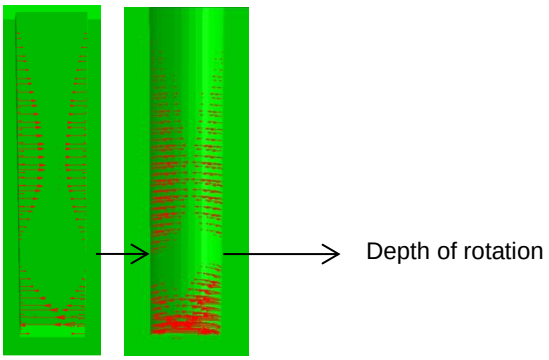

Figure 7. Lateral stresses acting on the soil body for the circular (right) and square (left) pile configurations

$$(E_p I_p)_{Hollow\ structure} = (E_p I_p)_{Solid\ structure} \quad (6)$$

$$(\rho A)_{Hollow\ structure} = (\rho A)_{Solid\ structure} \quad [7]$$

The results of the square pile/tower structure are not illustrated in Fig. 8 due to their very close agreement with the results of the circular structure. It is interesting to point out that the location (depth) of the maximum bending moments for the square structures at their ultimate lateral capacities is similar to the circular pile/tower structures for the FE and the theoretical solution.

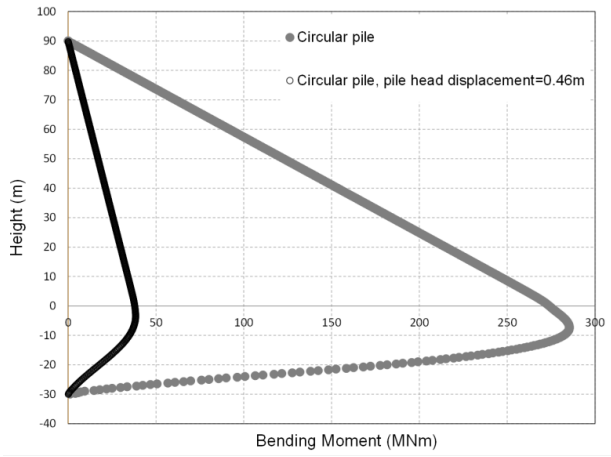

Figure 8. Bending moments acting on the circular pile/tower structure embedded in soil group B

Fig. 9 illustrates the lateral displacements extracted from the beam elements embedded at the center of the circular and square pile cross sections at their ultimate lateral capacities for soil groups A and B. The pivot point depth for the circular structures embedded in both soil groups A and B is at a depth of 23 m below the ground level while for the square structures (for both soil groups) the pivot point depth is at 22.5 m below the sea level. This illustrates that at the ultimate capacity, the pivot point depths of a circular and square pile structure are not equal and there is a slight difference in the depths of the pile's point of rotation.

Fig. 10 illustrates the same results for a tower head displacement of 0.23 m. The point of rotation for both pile configurations embedded in soil group A is at a depth of 21.5 m while for the square and circular piles installed in soil group B the pivot point depth is 21 m below the ground surface. The location of the pivot point moves towards the ground level as the soil stiffness increases (Pedram 2015) this point is evident in Fig. 10, but at the ultimate capacity (Fig. 9) this difference is not detected for each pile configuration installed in soil groups A and B; that is only the pile configuration effected the pile's pivot point depth and not the soil stiffness. The largest gap in the pile's pivot point depth between its ultimate state and a tower head displacement of 0.23 m is calculated for the circular structure embedded in soil group B and it is 2 m.

As discussed, by comparing the results of Figs. 9 and 10 it is clear that as the load acting on the tower's head reached the ultimate lateral capacity of the soil medium, the depth of the pivot point for the pile structures slightly increased. This point is similar to the increase in the location of the maximum bending moment when the structure approaches its ultimate lateral capacity.

To make sure that the increase in the pile's pivot point depth between tower head displacements of 0.23 m and the ultimate lateral capacity is not due to slippage of the pile at the ultimate state, the author followed the pivot point depth for the circular pile embedded in soil group A with changes made to the tower head displacement. It became evident that as the tower head displacement increased the depth of the pile's pivot point increased.

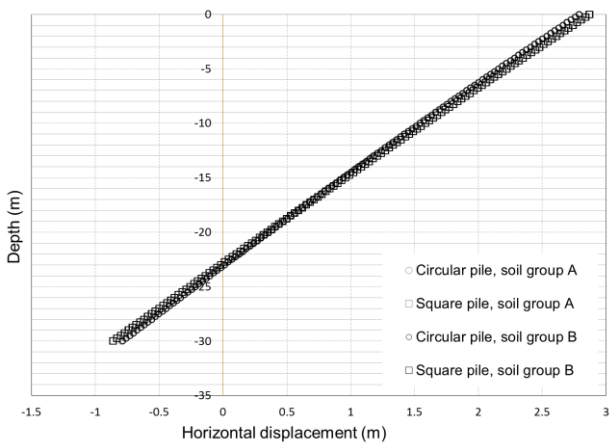

Figure 9. Lateral displacements at the center of the piles at the ultimate capacity for soil groups A and B

A parametric study was conducted to investigate the parameters affecting the pile's pivot point depth for a clay layer (a short-term analysis). It became evident that changes made to the soil modulus with the usual range of E_u/s_u = 350 to 1500 for clays do not influence the location of a pile's pivot point at the ultimate lateral capacity. Fig. 11 illustrates three sets of piles installed in clays at their ultimate capacities with different soil stiffness. It is clear that changes to the modulus (E_u) for a single pile case within the usual range do not affect the location of the pivot point of a pile structure at the ultimate capacity. In Fig. 11, within each set, the pile dimensions and properties are the same.

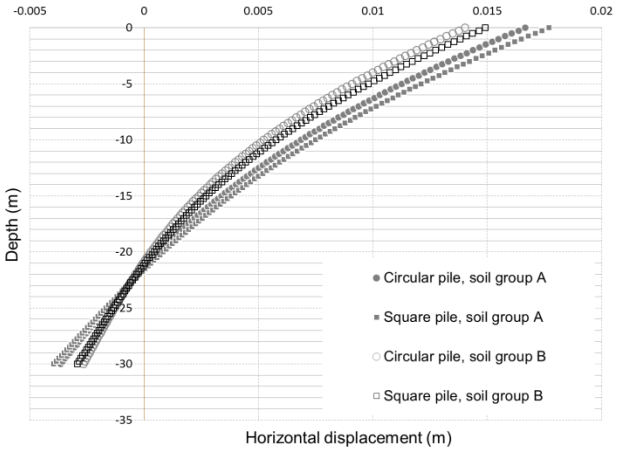

Figure 10. Lateral displacements of the pile centers at a tower head displacement of 0.23 m

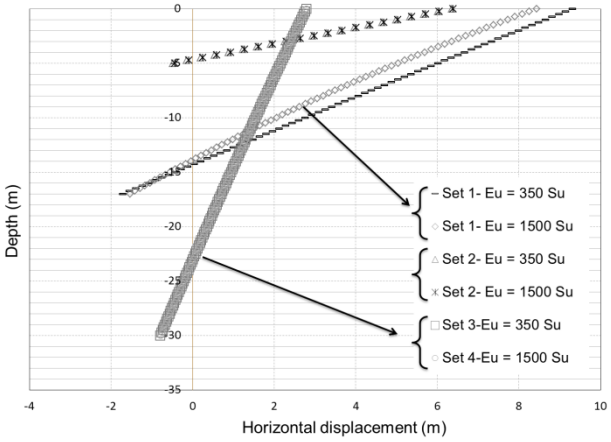

Figure 11. Effects of soil stiffness on the pivot point depth of piles in clays at their ultimate lateral capacities

5 CONCLUSION

Based on the results obtained from this investigation, the following conclusions are made with respect to the behavior of circular and square monopile structures embedded in soft normally consolidated offshore clay deposits.

It was apparent that the ultimate lateral capacity of the pile/tower structures embedded in a normally consolidated clay layer were controlled by soil failure and not by the structural capacity of the pile.

Although the ultimate lateral capacities of both pile/tower configurations were the same (soil failure controlled) it was evident that the stiffness of the square pile/tower structures embedded in both soil groups were higher than of a circular structure. The difference between the stiffness of the two pile/tower configurations could be above +30.0% at a tower head displacement of 0.46 m for soil group B. It was also illustrated that if structural failure occurred (a slightly overconsolidated clay layer) the stiffness and the ultimate lateral capacity of the square structures stand higher than of a circular pile/tower.

The location of the maximum bending moments on the circular pile/tower structure at the ultimate capacity and at a tower head displacement of 0.46 m were illustrated. It was clear that the location of the maximum bending moment extended further down the sea level as the lateral load on the tower increased. It was also illustrated that the method adopted by Murff and Hamilton (1993) was able to calculate both the ultimate lateral capacity and the location of the maximum bending moments generated on the pile structures accurately with respect to the FE analysis.

For a very soft soil medium, the depth of the pivot point of the pile slightly increased as the structure moved towards its ultimate lateral capacity. Moreover, for a short term analysis in clays, the depth of the structures pivot point was not influenced by the soil's stiffness for the range of E_u/s_u = 350 to 1500 at the ultimate lateral capacities.

6 REFERENCES

American Petroleum Institute (API) (2000). API recommended practice 2A-WSD (RP 2A-WSD) twenty-first edition, December 2000.

Broms, B. B. (1964). Lateral resistance of piles in cohesive soils, ASCE, Proc. Journal of Soil Mechanics and Foundation Division, Vol. 90(SM2), pp. 27-63.

Budhu, M. (2007). *Soil Mechanics and Foundations.* John Wiley & Sons.

Budhu, M. (2008). *Foundations and earth retaining structures.* John Wiley & Sons.

Budhu, M. and Davies, T.G. (1987). Nonlinear analysis of laterally loaded piles in cohesionless soils. Canadian Geotechnical journal, Vol. 24, 289-296.

Byrne, B.W., Houlsby, G.T. and Martin, C.M (2002). Cyclic loading of shallow offshore foundations on sand. *Proceedings of the International Conference on Physical modeling in Geotechics,* Newfoundland, Canada.

Cook, R.D., Malkus, D.S., Plesha, M.E. and Witt, R.J (2002). *Concepts and application of finite element analysis*. John Wiley & Sons.

Davies, T. G. and Budhu, M. (1986). Nonlinear analysis of laterally loaded piles in heavily overconsolidated clays. *Geotechnique*, Vol. 36 No. 4, pp. 527-538.

Dixon, R.K. (2005). *Marine Foundations*, Wo 2005/038146 (Patent application).

Fleming, W.G.K., Weltman, A.J., Randolph, M.F. and Elson, W.K. (1992). *Piling engineering*, University Press, pp 145-151.

Hibbeler, R.C. (2005). *Mechanics of Materials*, Prentice Hall.

Houlsby, G.T. and Byrne, B.W. (2005). "Calculation procedures for installation of suction caissons in sand," *J Geotechnical Engineering*, Vol. 158, pp 135-144.

Logan, D. L., Chaudhry, K. K. and Singh, P. (2011). *A first course in the finite element method*. Global Engineering.

Matlock, H. S. (1970). Correlations for design of laterally piles in soft clay. 2nd Annual Offshore Technology Conf., Houston, Texas

Mesri, G. (1975). Discussion: new design procedure for stability of soft clays. Journal of Geotechnical Engineering, ASCE, Vol. 101(GT4), 408-412.

Meyerhof, G.G. (1976). Bearing capacity and settlement of pile foundations. Journal of Geotechnical Engineering, ASCE, 102 (GT3), pp. 195-228.

Murff, J. D. & Hamilton, J. M. (1993). P-Ultimate for undrained analysis of laterally loaded piles, Journal of Geotechnical Engineering, ASCE, Vol. 119, No. 1, pp. 91-107.

Pedram, B. (2015). A numerical study on offshore wind turbines embedded in sands. Journal of Geotechnical Research. Vol. 2, No. 2, pp. 49-65.

Pedram, B. (2018). Behaviour of hybrid footing structures in sands. Journal of Geotechnical and Geological Engineering, Vol. 36, No.4, pp. 2273-2292.

Poulos, H.G. (1971). "Behavior of laterally loaded piles," Part I - single piles, *J Soil Mechanics and Foundation Division (ASCE)*, Vol. 97, No. SM5, pp 711-731.

Poulos, H.G., and Davis E.H. (1980). *Pile foundation analysis and design,* John Wiley & Sons.

Randolph, M. F. and Houlsby, G. T. (1984). The limiting pressure on a circular pile loaded laterally in cohesive soil, *Géotechnique*, 34 (4), pp.613-623.

Reese, L.C. (1958). Discussion of paper by B. McClelland and J. A. Focht. Trans. ASCE, 123:1071-1074.

Stone, K.J.L., Newson, T.A. and Sandon, J. (2007). "An investigation of the performance of a hybrid monopile-footing foundation for offshore structures," *Proc. 6th Int. Conf. of the society of Underwater Technology,* London, pp 391-396.

Ugural, A. C. 2007. *Mechanics of Materials*. John Wiley and sons.

Wang, D., Hu, Y. and Randolph, M.F. (2008). Three-dimensional large deformation analyses of plate anchor keying in clay. *Proc*. 27th International Conference on Offshore Mechanics and Arctic Engineering (*OMAE)*, Portugal.